Spatial Filtering of EEG Signals to Identify Periodic Brain Activity Patterns

Dounia Mulders[1,2(✉)], Cyril de Bodt[1], Nicolas Lejeune[2], André Mouraux[2], and Michel Verleysen[1]

[1] ICTEAM Institute, Université catholique de Louvain, Place du Levant 3, 1348 Louvain-la-Neuve, Belgium
{dounia.mulders,cyril.debodt,michel.verleysen}@uclouvain.be
[2] IONS Institute, Université catholique de Louvain, Avenue Mounier 53, 1200 Woluwe-Saint-Lambert, Belgium
{nicolas.lejeune,andre.mouraux}@uclouvain.be

Abstract. Long-lasting periodic sensory stimulation is increasingly used in neuroscience to study, using electroencephalography (EEG), the cortical processes underlying perception in different modalities. This kind of stimulation can elicit synchronized periodic activity at the stimulation frequency in neuronal populations responding to the stimulus, referred to as a steady-state response (SSR). While the frequency analysis of EEG recordings is particularly well suited to capture this activity, it is limited by the intrinsic noisy nature of EEG signals and the low signal-to-noise ratio (SNR) of some responses. This paper compares and adapts spatial filtering methods for periodicity maximization to enhance the SNR of periodic EEG responses, a key condition to generalize their use as a research or clinical tool. This approach uncovers both temporal dynamics and spatial topographic patterns of SSRs, and is validated using EEG data from 15 healthy subjects exposed to periodic cool and warm stimuli.

Keywords: Periodic Component Analysis · Spatial filtering
Generalized Rayleigh quotient · EEG · Thermal stimulation
Steady-states

1 Introduction

Understanding the neural mechanisms underlying human perception of stimuli from different modalities, such as visual, auditory, tactile or nociceptive, is a challenging issue in neuroscience. In this context, scalp electroencephalography (EEG) is particularly suited to record brain activity, as it is non-invasive and directly measures neuronal activity with a high temporal resolution of the millisecond order. Meanwhile, most studies consider brief sensory stimuli, lasting less than one second and eliciting well-known event-related potentials (ERPs) [10]. However, the recording of neural responses to long-lasting periodic

Y. Deville et al. (Eds.): LVA/ICA 2018, LNCS 10891, pp. 524–533, 2018.
https://doi.org/10.1007/978-3-319-93764-9_48

stimulation is increasingly proposed in several works as an alternative to probe sensory perception [2], since it reveals new aspects of the sensory information processing [8]. Such long-lasting stimuli indeed induce a periodic activity at the stimulation frequency in some neuronal populations. This so-called steady-state response (SSR) can usually be recorded with multichannel EEG.

One of the main advantages of the aforementioned periodic stimuli is that the signal-to-noise ratio (SNR) of the SSR is usually higher in the frequency domain compared to the time domain. Therefore, most neuroscience works up to now use frequency analyses to highlight the SSR features. The EEG time course and frequency transform at some specific electrodes can be studied, as well as the distribution across the scalp of the signal amplitude at the stimulation frequency. Although these approaches provide direct measures of the signal periodicity, their efficiency is limited when the SNR is low. For instance, this is the case with nociceptive SSRs generated from infrared laser stimulation [3]. In the meantime, whereas linear filtering methods have been successfully developed in the context of brain-computer interfaces (BCI) to classify steady-state visually evoked-potentials (SSVEP) [9,15], they were surprisingly not yet adapted to extract, interpret and characterize the EEG activity related to different periodic stimuli. Indeed, while the optimized filters can lead to high classification accuracies, their spatial patterns may also refine the analysis of SSRs.

In this context, this paper compares filtering methods maximizing the periodicity of the extracted components to study and, more importantly, interpret the cortical processing of periodic stimuli. The filters are constrained to be linear, thereby defining meaningful topographic patterns of the associated components. We propose to adapt four spatial filtering methods to enhance the SNR of SSRs. The two first methods are derived from a measure of periodicity in the time domain, first introduced by Saul and Allen [14]. This approach, called Periodic Component Analysis (πCA), was initially used to extract periodic components from speech signals. Variants have been developed, handling for instance non-strictly periodic signals such as the electrocardiogram [12]. A third method is based on Canonical Correlation Analysis (CCA) between the multichannel EEG signals and a relevant reference periodic signal [9]. Finally, the last method directly optimizes the spectral concentration of the filtered signals at the fundamental stimulation frequency and its harmonics.

This paper is organized as follows. Section 2 defines the compared methods in the context of our application. Section 3 presents empirical results validating the proposed methods on an EEG data set collected on 15 healthy subjects. Finally, Sect. 4 concludes and presents further perspectives.

2 Methods

This section introduces four methods aiming at extracting periodic components by filtering a noisy multidimensional signal $\mathbf{x}(t) \in \mathbb{R}^C$, assumed to have a zero-mean (i.e. $\sum_t \mathbf{x}(t) = 0$). Since the ultimate goal is to interpret the links between these components and the original signals, the spatial filters are constrained

to be linear and will be denoted by vectors $\mathbf{w} \in \mathbb{R}^C$. These filters are optimized to define a maximally periodic component $s(t) := \mathbf{w}^T\mathbf{x}(t)$ of fundamental frequency f_1 and corresponding fundamental period $T_1 = 1/f_1$. Once an optimal filter is found by optimizing a cost function F, a second optimal filter can be found, leading to a component in the orthogonal subspace of the first one. A matrix $W \in \mathbb{R}^{C\times d}$ is hence recursively built, whose columns are the filters ranked in decreasing order of periodicity of the filtered components as measured by F, which determines $d \leq C$. Pseudo-inverting the matrix $W^T \in \mathbb{R}^{d\times C}$ then estimates patterns of activity of the extracted components. Each filtered signal indeed has a fixed projection across the components of $\mathbf{x}$: writing the linear forward model as $\mathbf{x}(t) = A\mathbf{u}(t)$, with $\mathbf{u}(t) \in \mathbb{R}^{d\times 1}$ the periodic *sources*, estimates $W^T \approx A^{-1}$ are derived; the first column of $(W^T)^{-1}$ approximates the spatial pattern of the first estimated source signal $\mathbf{u}_1(t)$ [11].

2.1 Periodic Component Analysis

Periodic Component Analysis (πCA) [14] defines an optimal linear filter by minimizing a scale-invariant periodicity measure of the filtered signal $s(t) = \mathbf{w}^T\mathbf{x}(t)$:

$$\mathbf{w}_{\pi 1} = \arg\min_{\mathbf{w}} \left\{ F_{\pi 1}(\mathbf{w}) = \frac{\sum_t |s(t+T_1) - s(t)|^2}{\sum_t |s(t)|^2} = \frac{\mathbf{w}^T A_{\mathbf{x}}(T_1)\mathbf{w}}{\mathbf{w}^T C_{\mathbf{x}}(0)\mathbf{w}} \right\}, \quad (1)$$

where $A_{\mathbf{x}}(T_1) = \mathbb{E}_t\{(\mathbf{x}(t+T_1) - \mathbf{x}(t))\,(\mathbf{x}(t+T_1) - \mathbf{x}(t))^T\}$ and $C_{\mathbf{x}}(\tau) = \mathbb{E}_t\{\mathbf{x}(t+\tau)\mathbf{x}(t)^T\}$. The minimization of this generalized Rayleigh quotient is solved by the generalized eigenvalue decomposition (GEVD) of the matrix pair $(A_{\mathbf{x}}(T_1), C_{\mathbf{x}}(0))$. These two matrices being symmetric, the matrix of generalized eigenvectors W sorted in decreasing order of magnitude of the associated generalized eigenvalues gives the components $W^T\mathbf{x}(t)$ ranked in decreasing order of periodicity [4].

2.2 Periodic Component Analysis Variant

Another periodicity measure can alternatively be optimized as:

$$\mathbf{w}_{\pi 2} = \arg\max_{\mathbf{w}} \left\{ F_{\pi 2}(\mathbf{w}) = \frac{\sum_t |s(t+T_1)\cdot s(t)|}{\sum_t |s(t)|^2} = \frac{\mathbf{w}^T C_{\mathbf{x}}(T_1)\mathbf{w}}{\mathbf{w}^T C_{\mathbf{x}}(0)\mathbf{w}} \right\}. \quad (2)$$

This defines a variant [12] of πCA, denoted here by πCA_2. This problem can be similarly solved by a GEVD of the matrices $(C_{\mathbf{x}}(T_1), C_{\mathbf{x}}(0))$. It is noteworthy that whenever $C_{\mathbf{x}}(T_1)$ is symmetric, $A_{\mathbf{x}}(T_1) = 2\cdot(C_{\mathbf{x}}(0) - C_{\mathbf{x}}(T_1))$ and (2) is hence equivalent to (1). For any real-world signal $\mathbf{x}$ however, $C_{\mathbf{x}}(T_1)$ is unlikely to be symmetric. Therefore (1) and (2) will typically not define the same filters. Since (1) seems more generally suited for periodicity maximization, πCA is expected to outperform πCA_2 in the current application.

2.3 Canonical Correlation Analysis

Another approach to extract periodic components from a multidimensional signal is based on Canonical Correlation Analysis (CCA) [5]. The principle is to maximize the correlation between a filtered signal and a linear combination of the components of a reference signal $\mathbf{y}(t)$, with the same length as $\mathbf{x}$. In our setting, the components of $\mathbf{y}$ are defined from the Fourier series of a periodic signal of fundamental frequency f_1: $\mathbf{y}(t) = (\sin(2\pi f_1 t)\ \cos(2\pi f_1 t)\ \sin(2\pi 2 f_1 t)\ \ldots\ \sin(2\pi N_h f_1 t)\ \cos(2\pi N_h f_1 t))^T$, where N_h is a parameter indicating the number of accounted harmonics [9]. The CCA optimization problem is

$$(\mathbf{w}_{\pi 3}, \mathbf{w}_{\pi 3-y}) = \arg\max_{\mathbf{w},\mathbf{w}_y} \left\{ F_{\pi 3}(\mathbf{w}, \mathbf{w}_y) = \frac{\mathbf{w}^T C_{\mathbf{x};\mathbf{y}} \mathbf{w}_y}{\sqrt{\mathbf{w}^T C_{\mathbf{x}}(0)\mathbf{w} \cdot \mathbf{w}_y^T C_{\mathbf{y}}(0)\mathbf{w}_y}} \right\}, \quad (3)$$

where $C_{\mathbf{x};\mathbf{y}} = \mathbb{E}_t\{\mathbf{x}(t)\mathbf{y}(t)^T\}$. Only the optimal filter $\mathbf{w}_{\pi 3}$ is interesting in our context. The filter $\mathbf{w}_{\pi 3-y}$ being also optimized, (3) amounts finding the filtered signal $\mathbf{w}_{\pi 3}^T \mathbf{x}(t)$ which is maximally correlated with an arbitrary periodic signal whose frequency content is limited to $N_h f_1$. The solution to (3) is obtained by diagonalizing $C_{\mathbf{x};\mathbf{y}}$, $C_{\mathbf{x}}(0)$ and $C_{\mathbf{y}}(0)$ using only two matrices W and W_y with the filters in their columns [7].

2.4 Spectral Contrast Maximization

Spectral contrast maximization (SCM) consists in maximizing the magnitude of some frequency components of the filtered signal, with respect to the whole spectrum energy [13]. It is recommended when the searched components are more easily separable in the frequency domain, i.e. when the frequency band to amplify is known a priori. Let $S(f) := \mathcal{F}_f\{s(t)\} = \mathbf{w}^T \mathcal{F}_f\{\mathbf{x}(t)\} = \mathbf{w}^T X(f)$ denotes the Fourier transform of the filtered signal at frequency f. The optimal SCM filter is then defined as

$$\mathbf{w}_{\pi 4} = \arg\max_{\mathbf{w}} \left\{ F_{\pi 4}(\mathbf{w}) = \frac{\mathbb{E}_{f\in\nu}\{|S(f)|^2\}}{\mathbb{E}_{f\in\mu}\{|S(f)|^2\}} = \frac{\mathbf{w}^T S_{\mathbf{x}} \mathbf{w}}{\mathbf{w}^T C_{\mathbf{x}}(0)\mathbf{w}} \right\}, \quad (4)$$

with $\nu := \{\pm f_1, \pm 2f_1, \ldots, \pm N_h f_1\}$ the set of considered frequencies, μ the whole frequency range (the Nyquist band for discrete signals), $S_{\mathbf{x}} := \mathbb{E}_{f\in\nu}\{X(f)X(f)^*\}$ and using the Parseval's identity at the denominator. The set ν contains negative frequencies to ensure the realness of the cross-spectrum matrix $S_{\mathbf{x}}$. Again, N_h is the number of harmonics to consider, including the fundamental frequency. This problem is solved using the GEVD of $(S_{\mathbf{x}}, C_{\mathbf{x}}(0))$.

Although the two last methods are formulated differently, they are intrinsically related. Indeed, CCA maximizes the correlation of the filtered signal with an arbitrary sum of sines and cosines at the harmonic frequencies, while SCM maximizes the Fourier amplitudes of the filtered signal at the same frequencies. In both cases, normalization ensures a scale-invariance of the solutions.

3 Processing EEG Signals

The comparison of the performances of the methods introduced in Sect. 2 is conducted on an EEG data set, which is first described in Sect. 3.1. Section 3.2 defines the quality criterion employed to quantitatively compare the methods, and Sect. 3.3 finally summarizes the results.

3.1 Experimental Setting

We recorded scalp EEG on 15 healthy subjects to whom we applied sinusoidal stimulations with a thermal cutaneous stimulator (TCS) in 4 different conditions, as shown in Fig. 1: warm and cool with either a fixed or a variable active surface along the stimulation cycles. Five distinct zones of the TCS stimulation surface could indeed be controlled independently. These 4 conditions were chosen in order to determine, for both warm and cool stimuli, whether alternating the position of the active surface along the stimulation cycles could improve the SNR of the induced SSR. Varying the active surface is indeed likely to limit the response habituation, which can for instance be due to skin receptor fatigue. Each stimulus consisted in a 0.2 Hz sinusoidal waveform lasting 15 periods (i.e. 75 s) and was applied to the right forearm. Each subject received 12 trials from each condition, leading to 48 trials in total presented in a randomized order. To reduce artifacts, these 12 trials are averaged for each condition. The EEG was sampled at 1000 Hz and recorded using 64 electrodes placed on the scalp according to the international 10/10 system. All signals were high-pass filtered above 0.05 Hz to remove slow drifts (4^{th} order zero-phase Butterworth filter).

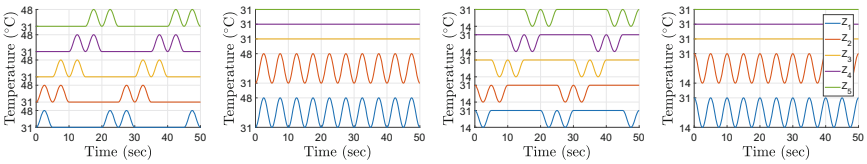

(a) w1 (b) w2 (c) c1 (d) c2

Fig. 1. Stimulation temperature profiles (only two thirds of the whole stimulus length of 75 s are shown for readability). Z_i means 'zone i' of the stimulator. w1 and w2 (resp. c1 and c2) indicate the two warm (resp. cool) conditions with a variable and fixed stimulation surface.

3.2 Quality Measure

In order to assess the quality of an extracted component, we define a periodicity measure for a given unidimensional signal $y(t)$ and fundamental frequency f_1. First, since each frequency amplitude $|Y(f)|$ is affected by some background noise, the average amplitude at 10 neighboring frequencies (5 higher and 5 lower) is removed from each frequency amplitude [8], resulting in a *noise-subtracted spectrum* $Y_{NS}(f) \in \mathbb{R}$. Then, the periodicity measure is defined as

$$M_\pi(y) = 100 \cdot \frac{\sum_{k=1}^{\lfloor f_s/(2\cdot f_1)\rfloor} Y_{NS}(k \cdot f_1)}{\sum_f |Y(f)|}, \tag{5}$$

with f_s the sampling frequency. In addition to accounting for the background noise, this measure is normalized with respect to the total signal amplitude. A positive (resp. negative) M_π suggests that the spectrum amplitude of y contains local maxima (resp. minima) on average at the harmonics $k \cdot f_1$. It is noteworthy that the components extracted using the methods from Sect. 2 should maximize this measure. Meanwhile, these methods are constrained to produce a linear filtering of the original signals, thereby providing topographical patterns of the extracted components which can be interpreted.

3.3 Periodic Components Extraction

Before analyzing the results obtained with the methods described in Sect. 2, we can observe whether the periodic components are visible in the raw EEG signals. The topographies of the Fourier transforms at $f_1 = 0.2$ Hz, shown in Fig. 2, suggest that the periodic components seem to be most prominent at centro-frontal electrodes, and in particular at FCZ (see Fig. 2b). The periodicity of the EEG signal at this location will hence be compared to the periodicity of filtered signals. The EEG time courses averaged over the stimulation periods as well as the spectra at this electrode are shown in Figs. 3 and 4 for all subjects. In both figures, the periodicity is visible for the warm conditions, while it is less clear for the cool ones, especially when the stimulation surface is fixed (condition c2). The average over the periods highlights more easily the periodic structure in the EEG, and in particular gives an estimate of the latency between the temperature and EEG peaks.

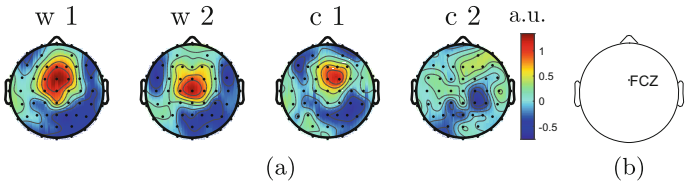

Fig. 2. Scalp topographies of (a) the group-level average noise-subtracted spectrum amplitudes at $f_1 = 0.2$ Hz and (b) the position of the FCZ electrode.

Performances of the periodicity-maximization methods are given in Table 1. First, the filter obtained from πCA, $\mathbf{w}_{\pi 1}$, outperforms the performances reached by $\mathbf{w}_{\pi 2}$. The poor results of $\mathbf{w}_{\pi 2}$ can partly be explained by the cross-channel symmetry hypothesis used to derive $F_{\pi 2}$ from $F_{\pi 1}$. Importantly, all filtering methods except πCA_2 lead to a filtered signal with an improved periodicity compared to the raw EEG signal at FCZ, even when this raw signal is hardly

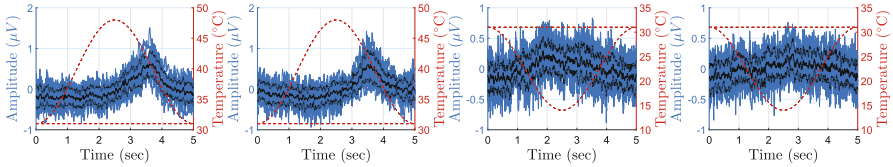

(a) w1 (b) w2 (c) c1 (d) c2

Fig. 3. EEG time courses averaged over the stimulation periods, at electrode FCZ for all 4 conditions. There is one curve per subject and the group-level average is in bold, with intervals of ± one standard deviation around the mean delimited with dotted lines. Dashed lines indicate the stimulation temperature.

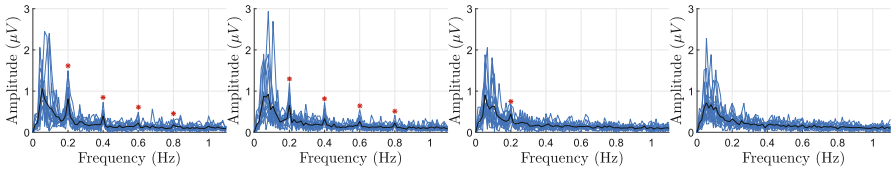

(a) w1 (b) w2 (c) c1 (d) c2

Fig. 4. EEG frequency spectrum at electrode FCZ for each subject and the 4 conditions. The group-level average is in bold. A star indicates significativity of the noise-subtracted peaks (Sect. 3.2) at $k \cdot f_1 = k \cdot 0.2$ Hz (paired t-test vs 0).

periodic, such as for condition c2 for instance, which corresponds to cool stimulations with a fixed stimulation surface. Two values of the parameter N_h are shown for CCA and SCM, chosen according to an analysis of the method performances as a function of N_h, not depicted here for space limitations. This analysis revealed a saturating increase of the performances which was consistent for all the conditions: as long as N_h is chosen higher than approximately 8, M_π has almost reached a plateau. The results of this table also indicate that:

- the SS responses obtained when stimulating the forearm with a variable surface (conditions w1 and c1) exhibit a more pronounced periodicity compared to the stimuli applied with a fixed surface (w2 and c2). The periodicity measure indeed shows this difference for almost all the filtered and raw signals.
- CCA and SCM extract the same periodic components (for all signals). This is not very surprising regarding the similarity between these two methods that was discussed in Sect. 2; a deeper algorithmic comparison is left for future works.
- performances of CCA and SCM are improved when the number of harmonics is increased, for all conditions. This further motivates the idea of extracting periodic non sinusoidal components instead of analyzing raw EEG frequency spectra: a single spatial pattern can regroup information from several harmonics.

The spatial patterns and filters obtained with the best filtering method (SCM with $N_h = 10$) are shown in Fig. 5. These spatial patterns indicate the distribution of the most periodic component across the scalp. The spatial filters on the other hand have more intricate scalp topographies than their associated patterns as they need to cancel the other interfering (noise) components [1]. In addition, the associated component time courses, averaged over the stimulation periods, and their Fourier transforms are given in Figs. 6 and 7, the y-scales of the latter differing from Fig. 4. These two last figures show the high periodicity of the filtered signals. This is in striking contrast with the raw signals at FCZ, especially for condition c2 depicted in Fig. 3d (with its spectrum in Fig. 4d), where no clear periodicity was visible. However, all methods rank, according to M_π, the components for each condition (i.e. the entries in each column of Table 1) in almost the same order as the FCZ signals (i.e. first column of Table 1), which encourages the valid interpretation of the filtered signal. Further validation will be conducted to ensure that the periodic amplified activity indeed reflects stimulation-related patterns. The average curves from Fig. 6 are also interesting as they show the time lag between the temperature peaks and the extracted part of the SSR. In particular, we observe a longer time lag for both warm conditions compared to the cool ones. This is in accordance with the fact that cool stimuli activate thinly-myelinated Aδ fibers [6], while the employed warm periodic stimuli most probably activate unmyelinated C fibers with slower conduction velocities [3].

Table 1. Mean(std) for the 15 subjects of the periodicity measure M_π of the components extracted with the periodicity-maximization methods of Sect. 2. For each stimulation type (row), the best performances are in bold. Italic characters indicate that the corresponding signal is not significantly less periodic than the best one of the same row. Significativity is computed with paired t-tests and is adjusted for multiple comparisons using the Holm-Bonferroni correction.

	FCZ signal	πCA	πCA$_2$	CCA		SCM	
				$N_h = 1$	$N_h = 10$	$N_h = 1$	$N_h = 10$
w1	1.02(0.49)	1.60(1.72)	−0.12(0.19)	2.84(1.20)	**3.04(1.15)**	2.84(1.20)	**3.04(1.15)**
w2	0.80(0.51)	1.50(1.65)	−0.12(0.18)	2.70(0.96)	**2.93(1.01)**	2.70(0.96)	**2.93(1.01)**
c1	0.19(0.24)	0.39(0.40)	−0.12(0.11)	1.99(0.56)	**2.17(0.57)**	1.99(0.56)	**2.17(0.57)**
c2	0.06(0.31)	0.44(0.51)	−0.11(0.14)	1.88(0.41)	**2.03(0.47)**	1.88(0.41)	**2.03(0.47)**

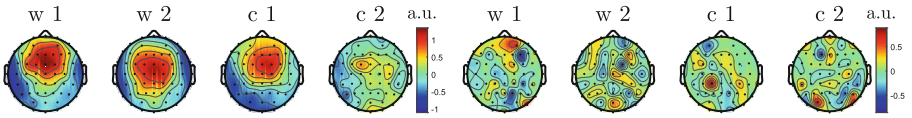

(a) Spatial patterns (b) Spatial filters

Fig. 5. Group-level average spatial patterns and spatial filters (defined at the beginning of Sect. 2) of the first component extracted with SCM ($N_h = 10$).

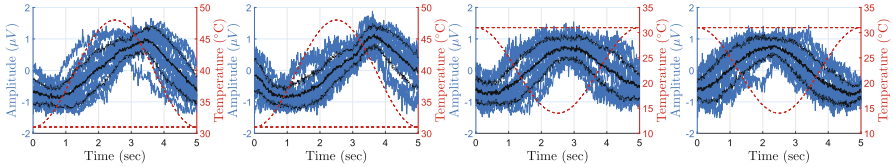

(a) w1 (b) w2 (c) c1 (d) c2

Fig. 6. Average over the stimulation periods of the optimal component extracted with SCM ($N_h = 10$). There is one curve per subject and the group-level average is in bold, with intervals of ± one standard deviation around the mean delimited with dotted lines. Dashed lines indicate the stimulation temperature.

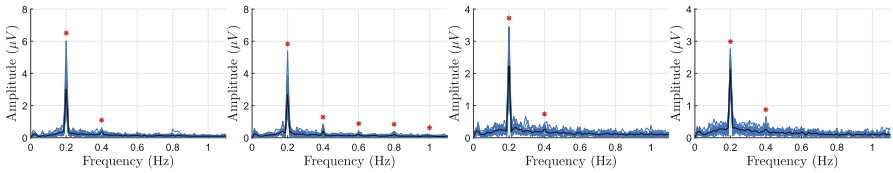

(a) w1 (b) w2 (c) c1 (d) c2

Fig. 7. Frequency spectrum of the components extracted with SCM ($N_h = 10$) for each subject. The group-level average is in bold. A star indicates significativity of the noise-subtracted peaks (Sect. 3.2) at $k \cdot 0.2$ Hz (paired t-test vs 0).

4 Conclusions and Perspectives

This paper suggests employing spatial filters to enhance the SNR of EEG responses elicited by periodic sensory stimulation. Four approaches are detailed and compared on an EEG data set recorded on 15 healthy subjects exposed to four different kinds of long lasting sinusoidal thermal stimuli. We show that these methods are able to extract periodic components from signals which do not necessarily exhibit a pronounced temporal periodicity. The estimated spatial activity patterns as well as the component time courses can hence characterize the steady-state responses.

As to further perspectives, the filtering methods considered in this work have been applied to the EEG signals averaged over the trials, enhancing their phase-locked components. Studying the periodic responses on a trial-basis, possibly using tensor methods, would enable determining whether and to which extent phase variability across trials affects the observed SSR. Another line of work is related to the analysis of the multiple suboptimal components, in terms of periodicity, extracted by the linear filters defined in Sect. 2. Whereas this paper focuses on the periodicity and spatial patterns of the optimal component identified by each method, it is very likely that the linear space spanned by the spatial patterns reflecting stimulation-related activity is more than one-dimensional in the studied EEG data. The considered linear filters moreover cannot compensate some phase changes across channels reflecting the propagation of the SSR

within brain regions. This hence suggests analyzing the links between the time dynamics of different filtered components and their spatial localization on the scalp.

Acknowledgments. DM and CdB are Research Fellows of the Fonds de la Recherche Scientifique - FNRS. The authors gratefully thank Prof. Christian Jutten for insightful discussions.

References

1. Blankertz, B., Lemm, S., Treder, M., Haufe, S., Müller, K.R.: Single-trial analysis and classification of ERP components-a tutorial. NeuroImage **56**(2), 814–825 (2011)
2. Colon, E., Legrain, V., Mouraux, A.: Steady-state evoked potentials to study the processing of tactile and nociceptive somatosensory input in the human brain. Neurophysiol. Clin./Clin. Neurophysiol. **42**(5), 315–323 (2012)
3. Colon, E., Liberati, G., Mouraux, A.: EEG frequency tagging using ultra-slow periodic heat stimulation of the skin reveals cortical activity specifically related to C fiber thermonociceptors. NeuroImage **146**, 266–274 (2017)
4. Golub, G.H., Van Loan, C.F.: Matrix Computations, vol. 3. JHU Press, Baltimore (2012)
5. Hardoon, D.R., Szedmak, S., Shawe-Taylor, J.: Canonical correlation analysis: an overview with application to learning methods. Neural Comput. **16**(12), 2639–2664 (2004)
6. Hüllemann, P., Nerdal, A., Binder, A., Helfert, S., Reimer, M., Baron, R.: Cold-evoked potentials-ready for clinical use? Eur. J. Pain **20**(10), 1730–1740 (2016)
7. Krzanowski, W.: Principles of Multivariate Analysis, vol. 23. OUP, Oxford (2000)
8. Mouraux, A., Iannetti, G.D., Colon, E., Nozaradan, S., Legrain, V., Plaghki, L.: Nociceptive steady-state evoked potentials elicited by rapid periodic thermal stimulation of cutaneous nociceptors. J. Neurosci. **31**(16), 6079–6087 (2011)
9. Nakanishi, M., Wang, Y., Wang, Y.T., Mitsukura, Y., Jung, T.P.: A high-speed brain speller using steady-state visual evoked potentials. Int. J. Neural Syst. **24**(06), 1450019 (2014)
10. Pfurtscheller, G., Da Silva, F.L.: Event-related EEG/MEG synchronization and desynchronization: basic principles. Clin. Neurophysiol. **110**(11), 1842–1857 (1999)
11. Samadi, S., Amini, L., Cosandier-Rimélé, D., Soltanian-Zadeh, H., Jutten, C.: Reference-based source separation method for identification of brain regions involved in a reference state from intracerebral EEG. IEEE Trans. Biomed. Eng. **60**(7), 1983–1992 (2013)
12. Sameni, R., Jutten, C., Shamsollahi, M.B.: Multichannel electrocardiogram decomposition using periodic component analysis. IEEE Trans. Biomed. Eng. **55**(8), 1935–1940 (2008)
13. Sameni, R., Jutten, C., Shamsollahi, M.B.: A deflation procedure for subspace decomposition. IEEE Trans. Sig. Process. **58**(4), 2363–2374 (2010)
14. Saul, L.K., Allen, J.B.: Periodic component analysis: an eigenvalue method for representing periodic structure in speech. In: Advances in Neural Information Processing Systems, pp. 807–813 (2001)
15. Wittevrongel, B., Van Hulle, M.M.: Frequency-and phase encoded SSVEP using spatiotemporal beamforming. PLoS One **11**(8), e0159988 (2016)